

Journal of
***Mechanics of
Materials and Structures***

OPTIMIZATION OF A SATELLITE WITH COMPOSITE MATERIALS

Jorge A. C. Ambrósio, Maria Augusta Neto and Rogério Pereira Leal

Volume 2, Nº 8

October 2007

OPTIMIZATION OF A SATELLITE WITH COMPOSITE MATERIALS

JORGE A. C. AMBRÓSIO, MARIA AUGUSTA NETO AND ROGÉRIO PEREIRA LEAL

The design of complex flexible multibody systems for industrial applications requires not only the use of powerful methodologies for the system analysis, but also the ability to analyze potential designs and to decide on the merits of each one of them. This paper presents a methodology using optimization procedures to find the optimal layouts of fiber composite structure components in multibody systems. The goal of the optimization process is to minimize structural deformation and to fulfill a set of multidisciplinary constraints. These methodologies rely on the efficient and accurate calculation of the system sensitivities to support the optimization algorithms. In this work a general formulation for the computation of the first order analytic sensitivities based on the direct differentiation method is used. The direct method for sensitivity calculation is obtained by direct differentiation of the equations defining the response of the structure with respect to the design variables. The equations of motion and the sensitivities of the flexible multibody system are solved simultaneously and, therefore, the accelerations and velocities of the system, and the sensitivities of the accelerations and velocities, are integrated in time using a multistep multiorder integration algorithm. Different models for the flexible components of the system, using beam and plate elements, are also considered. Finally, the methodology proposed here is applied to the optimization of the unfolding of a complex satellite made of composite plates and beams. The ply orientations of lamination are the continuous design variables. The potential difficulties in the optimization of composite flexible multibody systems are highlighted in the discussion of the results obtained.

1. Introduction

Modeling refers to the tools used in the construction of models of individual and coupled components of technical systems. The simplest models for multibody systems assume rigid body components while more complex models require the description of the components' flexibility. The finite element-based strategies used to represent the components' flexibility in multibody systems is a well accepted and widely used method. For systems in which the bodies are made of standard materials, there is a wide variety of finite elements that may be used, but when bodies are made of composite materials, the model flexibility often necessitates expensive finite element models with an inherent growth in complexity. Models of systems involving multibody dynamics methodologies also require a complete knowledge of the arrangement of the system components, which is achieved by the definition of kinematic joints, the introduction of models for external forces and the incorporation of the equilibrium equations of other disciplines [Heckmann et al. 2005; Møller et al. 2005; Bottasso et al. 2006]. Regardless of each particular type of joint used, the mathematical description of the restrictions involving only rigid bodies are the simplest to obtain. The presence of flexible bodies tends to increase the complexity of the description, and methods for simplifying the description are required [Lehner and Eberhard 2006; Hardeman et al.

Keywords: flexible multibody dynamics, sensitivity analysis, automatic differentiation, large rotations, floating frame.

2006]. However, the concept of virtual bodies provides a general framework for developing general kinematic joints for flexible multibody systems with minimal effort [Ambrósio 2003].

Analyses of rigid mechanical systems are the simplest and the least expensive, regardless of model. Flexible systems, in which the bodies only experience small elastic deformations, have higher computational costs. For these systems it is common to use mode component synthesis to reduce the number of generalized elastic coordinates and, consequently, the equations of motion are written in terms of modal coordinates [Nikravesh and Lin 2005; Gonçalves and Ambrósio 2005; Lehner and Eberhard 2006]. However, when the system components experience nonlinear deformations, the use of reduction methods is not possible, in general, and the finite element nodal coordinates are the generalized coordinates used [Ambrósio 1996; Dmitrochenko et al. 2006; Gerstmayr and Schöberl 2006; Vetyukov et al. 2006]. Furthermore, the analysis of these systems is more complex and, usually, computationally more expensive than the analysis of flexible systems with bodies that experience linear deformations.

In terms of the optimization complexity, the most complex and expensive problems are global or integer optimization problems with a large number of design variables. The simplest and cheapest problems to solve are continuous local problems with a small number of design variables [Venkataraman and Haftka 1999; Venkataraman and Haftka 2002]. Stochastic optimization algorithms, like simulated annealing methods or genetic algorithms, offer a way to perform global optimization, but they usually require several hundreds or even thousands of expensive simulation runs [He and Mcphee 2005; Kübler et al. 2005]. Eberhard and co-workers used a stochastic evolution strategy in combination with parallel computing in order to reduce the computation times while maintaining the inherent robustness [Eberhard et al. 2003]. Deterministic optimization algorithms, on the other hand, have a tendency to reach local minima, not necessarily the global optimum [Eberhard et al. 1999]. When supported by efficient calculation of the system sensitivities, these deterministic optimization algorithms often converge rapidly towards a local minimum with smaller computation times than other optimization approaches.

In this work, a general approach for sensitivity analysis of rigid-flexible multibody systems with composite materials based on the automatic differentiation method is used. The direct differentiation of the system equations of motion is obtained by the ADIFOR program [Bischof et al. 1992]. The dynamic equations and the time derivatives of the sensitivities are all integrated at the same time, thus the control of the time integration errors becomes more effective. The simultaneous integration of the equations is even more important when a variable step size or variable order integration algorithm is used, as is generally the case in multibody dynamic systems.

The optimization of the multibody composite components is performed by taking the ply orientations of lamination as continuous design variables. The multibody dynamic and sensitivities analysis code is linked with general optimization algorithms included in the package DOT/DOC [Vanderplaats 1992].

2. The multibody analysis methodology

2.1. Multibody equations of motion. The location of a rigid body is defined by the position of a body-fixed reference frame, $\xi\eta\zeta$, and its orientation with respect to an inertial frame, XYZ , as shown in Figure 1. The position and the orientation of the rigid body i is defined by the translation coordinates r_i and the rotational coordinates p_i . These coordinates are grouped in the vector $q_{r,i} = [r_i^T p_i^T]^T$. The coordinate vector of the complete flexible system is designated by $q = [q_r^T u'^T]^T$, which is composed

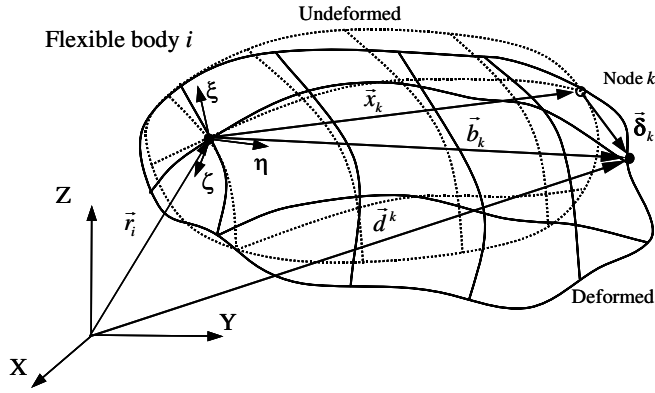


Figure 1. Flexible body with its body fixed coordinate system.

of the coordinate vector of the individual bodies and the elastic coordinates of the flexible bodies u'_i , generally the nodal coordinates of the finite element mesh measured with respect to the body-fixed coordinate system or the modal coordinates when a mode component synthesis method is used to represent the deformation of the flexible body.

For a multibody system, a set of constraint equations associated to the kinematic joints that restrict the relative motion between the bodies is defined as [Ambrósio and Gonçalves 2001]:

$$\Phi(q, t) \equiv \mathbf{0}, \tag{1}$$

where t refers to the kinematic constraints that depend on time. The constraints equations are added to the equilibrium equations using Lagrange multipliers

$$M\ddot{q} + \Phi_q^T \lambda = g + s - \underline{K}q, \tag{2}$$

where M is the system mass matrix, \underline{K} is the extended stiffness matrix of the system, g is a vector of external applied forces and s is the vector of the forces that depend on the square of the system velocities. Equation (2) includes n unknown accelerations and m unknown Lagrange multipliers associated with the algebraic constraint equations, but it only has n equations. The second time derivatives of the constraint equations provide the extra set of m equations necessary to support the solution of Equation (2). These acceleration constraint equations are

$$\ddot{\Phi}(\ddot{q}, \dot{q}, q, t) \equiv \Phi_q \ddot{q} - \gamma = \mathbf{0}. \tag{3}$$

Therefore, the complete system of equations that needs to be solved for a flexible multibody system is given by [Ambrósio and Gonçalves 2001]

$$\begin{bmatrix} M_r & M_{rf} & \Phi_{q_r}^T \\ M_{fr} & M_{ff} & \Phi_{q_f}^T \\ \Phi_{q_r} & \Phi_{q_f} & \mathbf{0} \end{bmatrix} \begin{Bmatrix} \ddot{q}_r \\ \ddot{u}' \\ \lambda \end{Bmatrix} = \begin{Bmatrix} g_r \\ g_f \\ \gamma \end{Bmatrix} - \begin{Bmatrix} s_r \\ s_f \\ \mathbf{0} \end{Bmatrix} - \begin{Bmatrix} \mathbf{0} \\ \underline{K}_{ff} u' \\ \mathbf{0} \end{Bmatrix}, \tag{4}$$

where \mathbf{K}_{ff} is the standard finite element stiffness matrix. The Jacobian matrix Φ_q^T and the right-hand-side vector $\boldsymbol{\gamma}$ of Equations (3) and (4) depend on the type of kinematic constraints used. The system equation matrix shows a large number of null elements and submatrix blocks of fixed size. The Markowitz sparse matrix solver is employed here to solve the system of equations defined by Equation (4) [Duff et al. 1986; Ambrósio 2003; Liu et al. 2007].

The equations of motion for the flexible multibody systems represented by (4) require a large number of coordinates to describe complex models. However, using component mode synthesis, the flexible body is described by a sum of selected modes of vibration as

$$\mathbf{u}' = \mathbf{X}\mathbf{w}, \tag{5}$$

where vector \mathbf{w} represents the contributions of the vibration modes towards the nodal displacements and \mathbf{X} is the modal matrix. Due to the reference conditions, the modes of vibration used here are constrained modes and due to the assumption of linear elastic deformations the modal matrix is invariant. The reduced equations of motion for the flexible body are [Ambrósio and Gonçalves 2001]

$$\begin{bmatrix} \mathbf{M}_r & \mathbf{M}_{rf}\mathbf{X} & \Phi_{q_r}^T \\ \mathbf{X}^T\mathbf{M}_{fr} & \mathbf{I} & \mathbf{X}^T\Phi_{q_f}^T \\ \Phi_{q_r} & \Phi_{q_f}\mathbf{X} & \mathbf{0} \end{bmatrix} \begin{Bmatrix} \ddot{\mathbf{q}}_r \\ \dot{\mathbf{w}} \\ \boldsymbol{\lambda} \end{Bmatrix} = \begin{Bmatrix} \mathbf{g}_r \\ \mathbf{X}^T\mathbf{g}_f \\ \boldsymbol{\gamma} \end{Bmatrix} - \begin{Bmatrix} \mathbf{s}_r \\ \mathbf{X}^T\mathbf{s}_f \\ \mathbf{0} \end{Bmatrix} - \begin{Bmatrix} \mathbf{0} \\ \boldsymbol{\Lambda}\mathbf{w} \\ \mathbf{0} \end{Bmatrix}, \tag{6}$$

where $\boldsymbol{\Lambda}$ is a diagonal matrix with the squares of the natural frequencies associated with the modes of vibration selected. The number of elastic coordinates in Equation (6) is equal to the number of vibration modes selected. For a more detailed discussion on the selection of the modes used, the interested reader is referred to [Cavin and Dusto 1977; Yoo and Haug 1986; Pereira and Proença 1991].

2.2. Flexible bodies made of composite materials. In this work the composite finite element used for the study of laminated plates is based on the Mindlin–Reissner plate theory, where only C^0 continuity is required for the approximation of the kinematic variables. At the element level and in local coordinates, the element stiffness matrix is given by [Neto et al. 2004]

$$\mathbf{K}_{ff}^{(e)} = \int_0^1 \int_0^{1-\eta} \begin{bmatrix} \mathbf{B}_m^T \mathbf{D}_m \mathbf{B}_m & \mathbf{B}_m^T \mathbf{D}_{mb} \mathbf{B}_b & \mathbf{0} \\ \mathbf{B}_b^T \mathbf{D}_{bm} \mathbf{B}_m & \mathbf{B}_b^T \mathbf{D}_b \mathbf{B}_b & \mathbf{0} \\ \mathbf{0} & \mathbf{0} & \mathbf{B}_s^T \mathbf{D}_s \mathbf{B}_s \end{bmatrix} |J| d\xi d\eta \tag{7}$$

which in a more compact form is written as

$$\mathbf{K}_{ff}^{(e)} = \int_0^1 \int_0^{1-\eta} (\mathbf{B}^T \mathbf{D} \mathbf{B})^{(e)} |J| d\xi d\eta. \tag{8}$$

The strain-displacement matrix is denoted by \mathbf{B} while \mathbf{D} is the elasticity matrix and $|J|$ is the determinant of the Jacobian matrix. The subscripts m , b and s stand for membrane, bending and shear. Because each layer may have different properties, the elasticity matrix \mathbf{D} is evaluated as a summation carried out over the thickness of all the layers. Therefore, equivalent single layer theories produce equivalent

stiffness matrices as weighted averages of the individual layer stiffness through the thickness. These matrices are dependent on each layer orientation, and are given by

$$\begin{aligned} (\mathbf{D}_m, \mathbf{D}_b, \mathbf{D}_{mb}, \mathbf{D}_s) &= \sum_{k=1}^n (\mathbf{D}_m, \mathbf{D}_b, \mathbf{D}_{mb}, \mathbf{D}_s)_k \\ &= \sum_{k=1}^n (\mathbf{C}_{3 \times 3}^1 H_1, \mathbf{C}_{3 \times 3}^1 H_2, \mathbf{C}_{3 \times 3}^1 H_3, \mathbf{C}_{2 \times 2}^2 H)_k \end{aligned} \quad (9)$$

with

$$H_n = \int_{h_{l-1}}^{h_l} (x_3^{n-1}) dz = \frac{1}{n} (h_{l+1}^n - h_l^n), \quad (10)$$

where h_i is defined in Figure 2. The axis x_3 is positive upward from the mid-plane of the plate. The L th layer is located between the points $x_3 = h_l$ and $x_3 = h_{l+1}$ in the direction of the thickness.

At the element level and in local coordinates, the consistent mass matrix is given by

$$\mathbf{M}_{ff}^{(e)} = \int_0^1 \int_0^{1-\eta} \rho^{(e)} (\mathbf{S}^T \mathbf{m} \mathbf{S})^{(e)} |\mathbf{J}| d\xi d\eta, \quad (11)$$

where \mathbf{m} is a matrix that contains the inertial terms, and ρ represents the specific mass of the element. Before the mass matrix given by Equation (11), is used in what follows, a procedure to obtain a diagonal mass matrix is applied [Cook 1987].

The description of some of the flexible bodies of the multibody systems requires the use of composite plates, discretized by triangular finite elements. The finite element is based in the theory described and has six degrees of freedom per node: $u_1^o, u_2^o, u_3^o, \phi_1, \phi_2$ and ϕ_3 . In the finite element mesh of some of the flexible bodies of the system composite beam elements are also used. For the sake of conciseness, none of these elements is described here, but for details on the formulations of the different composite finite elements, the interested reader is referred to [Neto et al. 2004].

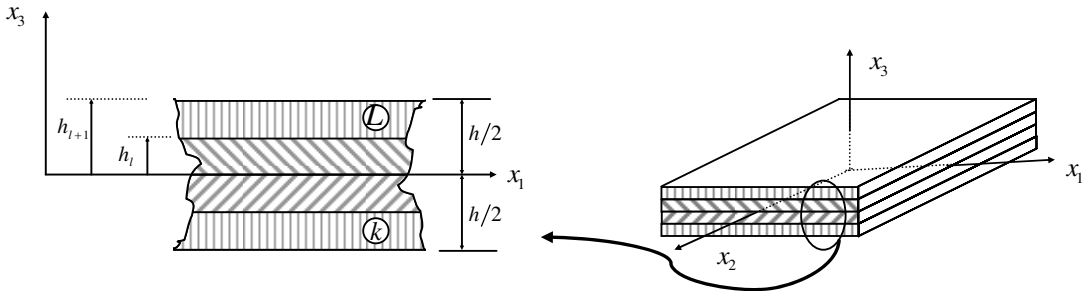


Figure 2. Coordinate system and layer numbering used for a typical laminated plate.

3. Sensitivity analysis of the multibody system

The optimization algorithms used in this work require not only the evaluation of the functional values of the behavior functions but also their sensitivities with respect to the design variables. The calculation of these sensitivities can be carried out analytically or numerically. In this work only the analytical sensitivities are obtained by using automatic differentiation.

3.1. Sensitivity of the equation of motion. For a rigid-flexible multibody system, the equations of motion in terms of modal coordinates are given by Equation (6). The sensitivities of the system accelerations and Lagrange multipliers with respect to the design variables are obtained by differentiating Equation (6) with respect to the design variables \mathbf{b} :

$$\begin{bmatrix} \mathbf{M}_r & \mathbf{M}_{rf}\mathbf{X} & \Phi_{q_r}^T \\ \mathbf{X}^T\mathbf{M}_{fr} & \mathbf{I} & \mathbf{X}^T\Phi_{q_f}^T \\ \Phi_{q_r} & \Phi_{q_f}\mathbf{X} & \mathbf{0} \end{bmatrix} \begin{Bmatrix} \ddot{\mathbf{q}}_{rb} \\ \ddot{\mathbf{w}}_b \\ \lambda_b \end{Bmatrix} = \begin{Bmatrix} \mathbf{Q}_b \\ \mathbf{R}_b \\ \gamma_b \end{Bmatrix}, \quad (12)$$

where $(\cdot)_b$ denotes the sensitivity of quantity (\cdot) with respect to \mathbf{b} . The sensitivities of the right-hand-side of the equation \mathbf{Q}_b , \mathbf{R}_b and γ_b are

$$\begin{aligned} \mathbf{Q}_b &= \frac{\partial}{\partial \mathbf{q}_r} (\mathbf{g}_r - \mathbf{S}_r - \mathbf{M}_r \ddot{\mathbf{q}}_r - \mathbf{M}_{rf} \mathbf{X} \ddot{\mathbf{w}} - \Phi_{q_r}^T \lambda) \mathbf{q}_{rb} + \frac{\partial}{\partial \dot{\mathbf{q}}_r} (\mathbf{g}_r - \mathbf{S}_r) \dot{\mathbf{q}}_{rb} + \frac{\partial}{\partial \dot{\mathbf{w}}} (\mathbf{g}_r - \mathbf{S}_r) \dot{\mathbf{w}}_b \\ &+ \frac{\partial}{\partial \mathbf{w}} (\mathbf{g}_r - \mathbf{S}_r - \mathbf{M}_r \ddot{\mathbf{q}}_r - \mathbf{M}_{rf} \mathbf{X} \ddot{\mathbf{w}} - \Phi_{q_r}^T \lambda) \mathbf{w}_b + \frac{\partial}{\partial \mathbf{b}} (\mathbf{g}_r - \mathbf{S}_r - \mathbf{M}_r \ddot{\mathbf{q}}_r - \mathbf{M}_{rf} \mathbf{X} \ddot{\mathbf{w}} - \Phi_{q_r}^T \lambda); \quad (13) \end{aligned}$$

$$\begin{aligned} \mathbf{R}_b &= \frac{\partial}{\partial \mathbf{q}_r} (\mathbf{X}^T \mathbf{g}_f - \mathbf{X}^T \mathbf{S}_f - \mathbf{X}^T \mathbf{K}_{ff} \mathbf{X} \mathbf{w} - \mathbf{X}^T \mathbf{M}_{fr} \ddot{\mathbf{q}}_r - \mathbf{X}^T \mathbf{M}_{ff} \mathbf{X} \ddot{\mathbf{w}} - \mathbf{X}^T \Phi_{q_f}^T \lambda) \mathbf{q}_{rb} \\ &+ \frac{\partial}{\partial \mathbf{w}} (\mathbf{X}^T \mathbf{g}_f - \mathbf{X}^T \mathbf{S}_f - \mathbf{X}^T \mathbf{K}_{ff} \mathbf{X} \mathbf{w} - \mathbf{X}^T \mathbf{M}_{fr} \ddot{\mathbf{q}}_r - \mathbf{X}^T \mathbf{M}_{ff} \mathbf{X} \ddot{\mathbf{w}} - \mathbf{X}^T \Phi_{q_f}^T \lambda) \mathbf{w}_b \\ &+ \frac{\partial}{\partial \mathbf{b}} (\mathbf{X}^T \mathbf{g}_f - \mathbf{X}^T \mathbf{S}_f - \mathbf{X}^T \mathbf{K}_{ff} \mathbf{X} \mathbf{w} - \mathbf{X}^T \mathbf{M}_{fr} \ddot{\mathbf{q}}_r - \mathbf{X}^T \mathbf{M}_{ff} \mathbf{X} \ddot{\mathbf{w}} - \mathbf{X}^T \Phi_{q_f}^T \lambda) \\ &+ \frac{\partial}{\partial \dot{\mathbf{q}}_r} (\mathbf{X}^T \mathbf{g}_f - \mathbf{X}^T \mathbf{S}_f) \dot{\mathbf{q}}_{rb} + \frac{\partial}{\partial \dot{\mathbf{w}}} (\mathbf{X}^T \mathbf{g}_f - \mathbf{X}^T \mathbf{S}_f) \dot{\mathbf{w}}_b; \quad (14) \end{aligned}$$

$$\begin{aligned} \gamma_b &= \frac{\partial}{\partial \mathbf{q}_r} (\gamma - \Phi_{q_r} \ddot{\mathbf{q}}_r - \Phi_{q_f} \mathbf{X} \ddot{\mathbf{w}}) \mathbf{q}_{rb} + \frac{\partial}{\partial \mathbf{w}} (\gamma - \Phi_{q_r} \ddot{\mathbf{q}}_r - \Phi_{q_f} \mathbf{X} \ddot{\mathbf{w}}) \mathbf{w}_b \\ &+ \frac{\partial}{\partial \mathbf{b}} (\gamma - \Phi_{q_r} \ddot{\mathbf{q}}_r - \Phi_{q_f} \mathbf{X} \ddot{\mathbf{w}}) + \frac{\partial \gamma}{\partial \dot{\mathbf{q}}_r} \dot{\mathbf{q}}_{rb} + \frac{\partial \gamma}{\partial \dot{\mathbf{w}}} \dot{\mathbf{w}}_b. \quad (15) \end{aligned}$$

After solving the linear system of Equations (12) to obtain the sensitivities $\ddot{\mathbf{q}}_{rb}$, $\ddot{\mathbf{w}}_b$ and λ_b the state variables' sensitivities are obtained by direct integration of $\dot{\mathbf{q}}_{rb}$, $\dot{\mathbf{w}}_b$, $\dot{\mathbf{q}}_{rb}$ and $\dot{\mathbf{w}}_b$. The process is started

with the initial conditions given by:

$$\begin{cases} \mathbf{q}_{r_b}(t_0) = \mathbf{q}_{r_b}^0, \\ \mathbf{w}_b(t_0) = \mathbf{w}_b^0, \\ \dot{\mathbf{q}}_{r_b}(t_0) = \dot{\mathbf{q}}_{r_b}^0, \\ \dot{\mathbf{w}}_b(t_0) = \dot{\mathbf{w}}_b^0. \end{cases} \quad (16)$$

Generally, the initial conditions for the sensitivities expressed in Equation (16) are assumed to be null. Note also that the leading matrix of (6) is equal to the leading matrix of Equation (12). Generally, the factorized matrix used to obtain the solution of the equation of motion does not have to be calculated again when the sensitivities system of equations need to be solved. However, because an automatic differentiation tool is used [Bischof et al. 1996], the subroutine that computes the solution of the system equations of motion is differentiated in order to obtain the sensitivity of the solution vector. The differentiated version of the subroutine is not only used to compute the sensitivities solution vector, but also to evaluate the derivative of the algorithm by which the solution is computed. The system accelerations ($\ddot{\mathbf{q}}_r, \ddot{\mathbf{w}}$) and the sensitivity solution vector of Equation (6), ($\ddot{\mathbf{q}}_{r_b}, \ddot{\mathbf{w}}_b$), are obtained simultaneously.

Due to the coordinate reduction, which uses component mode synthesis, the nodal displacements of the flexible body are described by Equation (5). The sensitivity of the nodal displacement is obtained by computing the derivative of this equation with respect the design variables written as

$$\frac{d\mathbf{u}'}{d\mathbf{b}} = \frac{\partial \mathbf{X}}{\partial \mathbf{b}} \mathbf{w} + \mathbf{X} \frac{\partial \mathbf{w}}{\partial \mathbf{b}} = \mathbf{X}_b \mathbf{w} + \mathbf{X} \mathbf{w}_b, \quad (17)$$

where \mathbf{X}_b are the sensitivities of the eigenmodes. The relation expressed in Equation (17) transforms the modal sensitivities to nodal sensitivities. Haftka and Gürdal [1992] suggests evaluating this transformation by the fixed-mode approach, in which the derivatives of vibration modes are neglected, or by the updated-mode approach, where the derivatives of vibration modes are accounted for. The fixed-mode approach is computationally less expensive but the updated-mode approach can occasionally be more accurate. The right-hand side of Equation (12) also depends on the sensitivities of the eigenmodes. Therefore, the same approach is used in the computation of the derivatives of the modal forces and in the derivatives of the modal stiffness matrix. The modal stiffness matrix derivative is computed in the updated-mode approach by

$$\frac{\partial}{\partial \mathbf{b}} (\mathbf{X}^T \mathbf{K}_{ff} \mathbf{X}) = \frac{\partial \mathbf{X}^T}{\partial \mathbf{b}} \mathbf{K}_{ff} \mathbf{X} + \mathbf{X}^T \frac{\partial \mathbf{K}_{ff}}{\partial \mathbf{b}} \mathbf{X} + \mathbf{X}^T \mathbf{K}_{ff} \frac{\partial \mathbf{X}}{\partial \mathbf{b}}, \quad (18)$$

while in the fixed-mode approach, it is obtained as

$$\frac{\partial}{\partial \mathbf{b}} (\mathbf{X}^T \mathbf{K}_{ff} \mathbf{X}) = \mathbf{X}^T \frac{\partial \mathbf{K}_{ff}}{\partial \mathbf{b}} \mathbf{X}. \quad (19)$$

The computation of the sensitivities of the eigenmodes is done using the Nelson scheme in the case of distinct eigenvalues. However, when repeated eigenvalues are a possibility, Ojavo's method is used [Dailey 1989].

3.2. Derivative of the element stiffness matrix. In this work, the design variables used for the laminate optimization problem are the fiber angles of each lamina that make up the laminate, denoted by vector θ . Therefore, the derivative of the stiffness matrix of the composite flexible body with respect to the layers' orientations has to be accounted for. At the element level, in local coordinates, the stiffness matrix is given by Equation (8). In this equation, only the matrix \mathbf{D} depends on the design variables. Thus, the sensitivity of this equation is given by

$$\frac{\partial \mathbf{K}_{ff}^{(e)}}{\partial \mathbf{b}} = \int_0^1 \int_0^{1-\eta} \left(\mathbf{B}^T \frac{\partial \mathbf{D}}{\partial \mathbf{b}} \mathbf{B} \right)^{(e)} |\mathbf{J}| d\xi d\eta. \tag{20}$$

The elasticity matrix \mathbf{D} depends on the submatrices \mathbf{D}_m , \mathbf{D}_b , \mathbf{D}_{mb} and \mathbf{D}_s , which are defined by Equation (9). The partial derivative of Equation (9) with respect to the design variables vector is

$$\begin{aligned} (\mathbf{D}_m, \mathbf{D}_b, \mathbf{D}_{mb}, \mathbf{D}_s)_b &= \left(\sum_{k=1}^n (\mathbf{D}_m, \mathbf{D}_b, \mathbf{D}_{mb}, \mathbf{D}_s)_k \right)_b \\ &= \sum_{k=1}^n (\mathbf{C}_{3 \times 3b}^1 H_1, \mathbf{C}_{3 \times 3b}^1 H_2, \mathbf{C}_{3 \times 3b}^1 H_3, \mathbf{C}_{2 \times 2b}^1 H)_k \end{aligned} \tag{21}$$

with

$$(\mathbf{C}_b)_k = \left(\frac{\partial \mathbf{T}^T}{\partial \mathbf{b}} \bar{\mathbf{C}} \mathbf{T} + \mathbf{T}^T \frac{\partial \bar{\mathbf{C}}}{\partial \mathbf{b}} \mathbf{T} + \mathbf{T}^T \bar{\mathbf{C}} \frac{\partial \mathbf{T}}{\partial \mathbf{b}} \right)_k. \tag{22}$$

In Equation (22) $(\bar{\mathbf{C}}_b)_k$ is the sensitivity of the material matrix of elastic coefficients for the layer k expressed in the local body frame, and $(\partial \mathbf{T} / \partial \mathbf{b})_k$ is the sensitivity of the transformation matrix relative to the design variables. Matrix \mathbf{T} represents the transformation between the local body frame and the material coordinate systems for layer k . The element mass matrix does not depend on the design variables therefore the partial derivative of this matrix with respect the design variables is null.

4. Optimization criteria

The different optimization problems in multibody systems lead, in general, to different criteria functions and design constraints. The objective functions most widely used in multibody problems are of one of two types: maximum or minimum values and the integral type. Consider a general multibody response defined by function $f_0(\mathbf{b}, \mathbf{z}, \boldsymbol{\lambda}, t)$, which is dependent on time and on the state and design variables. In multibody systems, all the terms present in the equations of motion may be functions of the design parameters. In a compact form the problem objective functions are given by Chang and Nikravesh [1985]:

$$\Psi_i = \Psi_i(\mathbf{b}, \mathbf{z}, \boldsymbol{\lambda}, t), \quad i = 0, \dots, n, \tag{23}$$

where the state vector \mathbf{z} includes the coordinates, velocities and accelerations. The variables of the state vector may depend on time and on the design variables. Therefore, the dependency of the state variables on the design variables and time is explicitly written as

$$\mathbf{z}(\mathbf{b}, t) = (\mathbf{q}(\mathbf{b}, t), \dot{\mathbf{q}}(\mathbf{b}, t), \ddot{\mathbf{q}}(\mathbf{b}, t)). \tag{24}$$

The dependencies of the state variables on the design variables are explicitly taken into account by the automatic differentiation tool that uses the chain rule to calculate the sensitivities.

4.1. Mini-max optimization problem. The min-max optimization problem, for the time interval between t_i and t_e is stated as

$$\text{minimize } \Psi_0^{\max} = \max f_0(\mathbf{b}, \mathbf{z}, \boldsymbol{\lambda}, t), \quad t_i \leq t \leq t_e, \quad (25)$$

where the problem consists in the minimization of the maximum value of a specific function during a given time interval. The use of the maximum value of a time dependent function response as the objective function makes it a more difficult problem to solve. This type of objective function may appear, for instance, when the minimization of the maximum value of acceleration or force in a given point of a body is required during dynamic analysis. In this optimization problem two situations can occur:

- (1) The instant in which the function is at the maximum value is unique and perfectly defined. In this case, during the optimization process the instant t_m is not dependent on the design variables, and therefore the objective function (25) can be replaced by a simpler objective function as

$$\text{minimize } \Psi_0^{\max} = \max f_0(\mathbf{b}, \mathbf{z}(t_m), \boldsymbol{\lambda}(t_m)). \quad (26)$$

- (2) The instant in which the function is at the maximum value, varies during the optimization process. One form of dealing with this problem is to introduce an extra design variable and make the objective function equal to the value of that variable [Haftka and Gürdal 1992; Kim and Choi 1996]:

$$\text{minimize } \Psi_0 = b_{n+1} \quad (27)$$

with the additional time-dependent constraint

$$\Psi_{n+1} = f_0(\mathbf{b}, \mathbf{z}, \boldsymbol{\lambda}, t) - b_{n+1} \leq 0, \quad t_i \leq t \leq t_e. \quad (28)$$

The constraint given by Equation (28), when added to the total number of constraints ensures, that the dynamic response is below the maximum value defined by the auxiliary variable b_{n+1} . This approach poses some difficulties for the search direction in the optimization algorithm and can lead to small steps in the line search method, or even to a stall of the process. To overcome these difficulties, Kim and Choi [1996] proposed to handle directly the maximum value point only in the optimization process.

4.2. Minimization of an integral type criteria. The integral type objective function may be used to represent mean values of the response over time, accumulated values, or other special criteria. For a response $f_0(\mathbf{b}, \mathbf{z}, \boldsymbol{\lambda}, t)$ of the dynamic system, the objective function is [Eberhard et al. 2003]

$$\Psi_0 = G_0(\mathbf{b}, \mathbf{z}_{t_e}, \boldsymbol{\lambda}_{t_e}, t_e) + \int_{t_i}^{t_e} f_0(\mathbf{b}, \mathbf{z}, \boldsymbol{\lambda}, t) dt, \quad (29)$$

where $f_0(\mathbf{b}, \mathbf{z}, \boldsymbol{\lambda}, t)$ depends on the dynamic behavior during the complete time interval $[t_i, t_e]$, while G_0 considers only the final state. This type of objective function is most common in vehicle design. Comfort or injury criteria are defined by integral type functions and often are used in the optimization process.

4.3. Time-dependent constraints. Mathematical programming algorithms generally cannot deal with parametric constraints such as

$$\Psi_i = f_i(\mathbf{b}, \mathbf{z}(t), \boldsymbol{\lambda}(t), t) \leq c, \quad t_i \leq t \leq t_e, \quad (30)$$

or even with constraints such as the one described by Equation (28). Such constraints have to be reformulated to remove their time dependency. During the simulation the function value can only be obtained for discrete time points. The most straightforward way to remove the time dependency of the original constraint is to discretize the time interval into time points. Then, the original constraint represented by Equation (30) is replaced by n_{tp} constraints written as [Haug and Arora 1979]:

$$\Psi_i = f_i(\mathbf{b}, \mathbf{z}(t_k), \boldsymbol{\lambda}(t_k), t_k) \leq c, \quad k = 1, \dots, n_{tp}. \quad (31)$$

The distribution of the time points has to be sufficiently dense to avoid large constraint violations between two adjacent time points [Hsieh and Arora 1984]. Thus, discretizing time-dependent constraints can significantly increase the number of constraints, and thereby the cost of optimization [Haftka and Gürdal 1992]. In order to reduce the number of constraints, a first alternative consists of replacing the original constraints by an equivalent integrated constraint, which averages the severity of the constraint over the time interval. Hsieh and Arora [1984] showed that from an optimization theory point of view, the constraints described by Equation (30) and equivalent integral constraints are different. In fact, an equivalent integral constraint represents the behavior of the time dependent constraint $f_i(\mathbf{b}, \mathbf{z}(t), \boldsymbol{\lambda}(t), t)$ on the complete time domain by a single value Ψ_i^e , leading to a loss of information. As a consequence, equivalent constraints tend to blur the design trends [Haftka and Gürdal 1992]. Hsieh and Arora [1984] and Grandhi et al. [1986] propose an alternative procedure that consists of exchanging the initial constraint given by (30) for a set of constraints of the type of Equation (31), in which n_{tp} is replaced by n_{ctp} , with $n_{ctp} < n_{tp}$ being n_{ctp} the number of critical time points. These critical points are related with the existence of local maxima or minima of the function.

5. Optimization algorithms

In dynamic problems the evaluation of the system dynamic behavior requires the numerical integration of the equation of motion. The time dependency of this system makes these optimization problems more complex and requires that special techniques be used in the solution process. Both deterministic and stochastic optimization methods can be applied. Eberhard et al. [2003] has successfully used a stochastic evolution strategy in combination with a parallel computing environment to reduce computation time. However, in this work the Modified Method of Feasible Directions is used, which is a deterministic optimization method implemented in the DOT optimization routines library [Vanderplaats 1992]. In order to calculate the gradients, the direct differentiation method is used, the sensitivities being obtained by the automatic differentiation program ADIFOR [Bischof et al. 1996].

6. Optimization of a satellite unfolding process

The proposed methodology is demonstrated through the optimization of a complex multibody system made of composite material. The technical system modeled within this application consists in the unfolding process of a satellite antenna, the Synthetic Aperture Radar (SAR) antenna, which is a part of

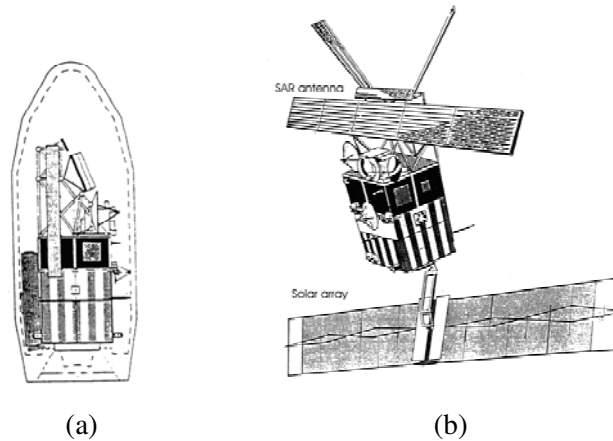


Figure 3. The SAR antenna in the (a) folded and (b) unfolded configurations.

the European research satellite ERS-1. The model of this antenna has been the object of different studies in several studies in multibody dynamics being first proposed by Hiller [1983] and Anantharaman and Hiller [1991].

6.1. Description of the SAR antenna. The folding antenna shown in Figure 3 is achieved through a relatively complex spatial mechanism. Both the solar array and the SAR antenna of the ERS-1 satellite have the same configuration and share the same kinematic features. During transportation the antenna and the solar array are folded, as shown in Figure 3a, in order to occupy as small a space as possible. After unfolding, the mechanical components take the configuration represented in Figure 3b.

The SAR antenna consists of two identical subsystems, each with three coupled planar four-bar links that unfold two panels on each side. The central panel is attached to the main body of the satellite. Each unfolding system has two degrees of freedom, driven individually by actuators located in the joints A and B, shown in Figure 4.

The unfolding process consists of two phases, schematically represented in Figure 5. In the first phase the panel 3 is rolled out, about an axis normal to the main body, by a rotational spring-damper-actuator in joint A, while the panel 2 is held down by locking joints D and E, as shown in Figure 5a. The second phase begins with joint A locked, the panels 2 and 3 being swung out to the final position by a rotational

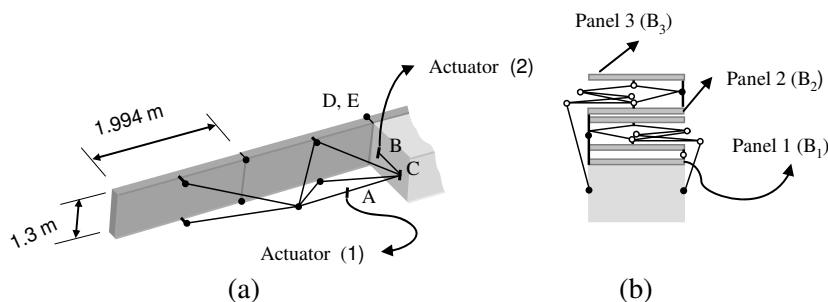


Figure 4. The SAR antenna: (a) one half unfolded state; (b) folded antenna.

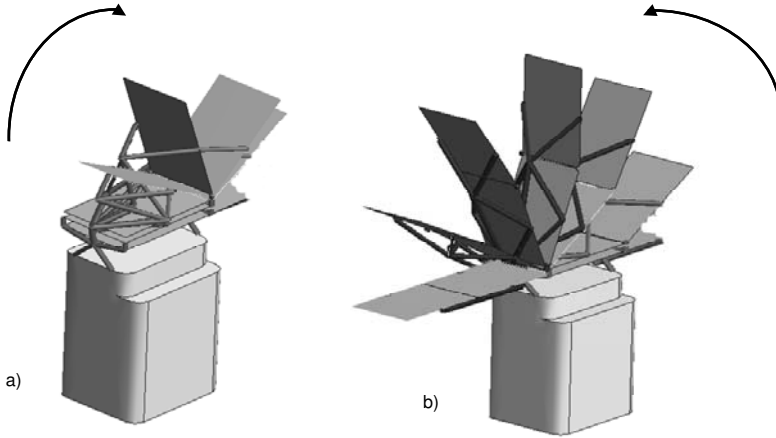


Figure 5. Unfolding process of the SAR antenna: (a) first phase; (b) second phase.

spring-damped-actuator in joint B, as observed in Figure 5b. The second half of the antenna, which has been omitted in Figures 4 and 5, is unfolded in the same way as the first half shown here. When the complete antenna is deployed all five panels are aligned in the final configuration.

The model used for one half of the folding antenna, schematically depicted Figure 6, is composed of 12 bodies (B_1 a B_{12}), 16 spherical joints (S_1 a S_{16}) and 3 revolute joints (R_1 , R_2 , R_3). The central panel is attached to the satellite, defined as body B_1 , which has mass and inertias much higher than the remaining bodies.

In the first phase of the unfolding antenna a rotational spring-damper-actuator is applied to the revolute joint R_3 . For the second phase, the revolute joint R_3 is locked and the system is moved to the next equilibrium position by a spring-damper-actuator positioned in joint R_1 . Each panel is 1.994 m long by 1.3 m wide and has a thickness of 2 mm. The linkage between the panels and the four-bar linkage mechanism is assured by a set of supports, six in body 2 and four in body 3. All truss members have a uniform circular cross-section [Neto 2005].

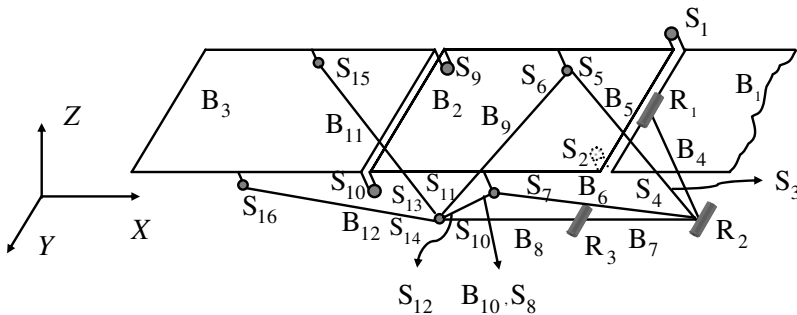


Figure 6. Multibody model of the SAR antenna.

	1st Layer	2nd Layer	3rd Layer	4th Layer
Lay-up 1	0°	0°	0°	0°
Lay-up 2	0°	90°	90°	0°
Thickness (m)	0.0005	0.0005	0.0005	0.0005

Table 1. Characteristics of the two lay-ups considered for the composite panels.

6.2. First phase of the antenna unfolding process. The material used in the different components of the antenna is a carbon reinforced plastic IM6/SC1081 where the matrix is made of Epoxy SC1081 and the fibers are made of Carbon IM6. Note that the material model used here is not necessarily that of the real satellite antenna, as the characteristics of the material are not publicly available. The properties of the composite material, for a single layer with an orientation of 0° relative to the X axis are: $E_1 = 177$ GPa; $E_2 = 10.8$ GPa; $G_{12} = G_{13} = 7.6$ GPa; $G_{23} = 8.504$ GPa; $\nu_{12} = 0.27$; with a specific mass of 1600 Kg/m³. Two different laminates with four layers in each, described in Table 1, are considered as potential design solutions.

In flexible multibody models the use of all the nodal degrees of freedom, resulting from the model of the complex system, as generalized coordinates is not viable. The application of the modal superposition technique in this kind of problem, characterized by linear elastic deformations, can be done without compromising accuracy. By using of a small set of the modes of vibration associated to the lower frequencies it is possible to reproduce the structural deformations of the panels with a small number of generalized elastic coordinates.

The modes of vibration for all flexible bodies in the antenna are obtained by performing a modal analysis of each one of the flexible bodies independently. The structural attachment conditions used in the eigenproblem are the same as those used to fix the body coordinate system, that is, the node in the center of mass is fixed to the body fixed frame. In this manner the free rigid body modes are removed.

In Tables 2 and 3 the 14 lowest frequencies are presented for panels 2 and 3 with composite material lay-ups 1 and 2, respectively. The modes corresponding to the two lower frequencies are almost rigid modes, resulting from the flexibility around a fixed node. However, these modes also represent deformation of the panels and cannot be neglected.

The actuator that is applied in revolute joint R_3 , to initiate the satellite unfolding process, is modeled as a nonlinear spring and damper actuator. The spring-damper-actuator is described by piecewise-linear characteristics given by:

$$M(\theta, \dot{\theta}) = c\dot{\theta} + \begin{cases} 0.10 + 9.00(3.12 - \theta) & 3.08 < \theta \leq 3.12 \\ 0.45 + 60.41(3.08 - \theta) & 3.02 < \theta \leq 3.08 \\ 4.03 - 5.19(3.02 - \theta) & 2.63 < \theta \leq 3.02 \\ 2.00 & 0.20 < \theta \leq 2.63 \\ 10.00\theta & -0.20 \leq \theta \leq 0.20 \\ -2.00 & -0.20 > \theta, \end{cases} \quad (32)$$

Mode	Panel 2 Frequency [Hz]	Panel 3 Frequency [Hz]
1	0.990	0.992
2	1.457	1.460
3	1.677	1.681
4	1.746	1.749
5	4.000	4.001
6	4.609	4.620
7	6.099	6.118
8	6.814	6.850
9	8.538	8.564
10	8.578	8.583
11	12.434	12.451
12	12.828	12.833
13	14.354	14.404
14	14.415	14.485

Table 2. First 14 natural modes of vibration for panels 2 and 3 with the composite material lay-up 1.

Mode	Panel 2 Frequency [Hz]	Panel 3 Frequency [Hz]
1	1.311	1.313
2	1.563	1.566
3	1.694	1.699
4	2.334	2.336
5	4.719	4.719
6	5.755	5.770
7	6.220	6.242
8	7.388	7.427
9	12.832	12.844
10	12.953	12.971
11	13.626	13.685
12	13.829	13.873
13	15.282	15.303
14	15.969	15.986

Table 3. First 14 natural modes of vibration for panels 2 and 3 with the composite material lay-up 2.

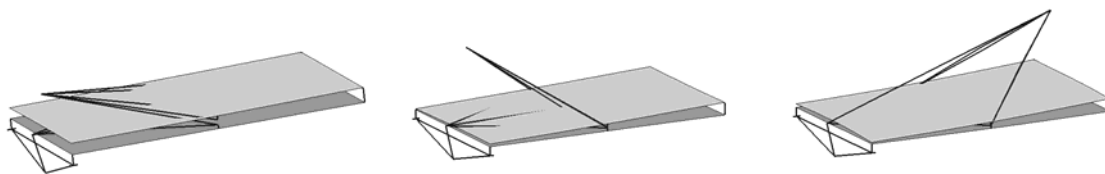


Figure 7. Configuration of the composite panels with the original damped spring-actuator.

where the damping coefficient used is $c = 0.5 \text{ Nms}$.

The actuation law presented here is different from that reported by Anantharaman and Hiller [1991], which was used to model the SAR antenna with panels made of isotropic material. In fact, when the actuation law used by Anantharaman and Hiller is used for the composite flexible models the satellite antenna is driven to a different equilibrium state than that obtained in the rigid model. The trusses connected to the actuator quickly reach their equilibrium, but panel 3 hardly moves because the unfolding trusses break through the panel, as represented in Figure 7. This behavior is clearly unfeasible because contact between trusses and panels would take place, preventing such penetration from happening. Therefore, the reported results show that due to the deformations of the trusses the undesirable contacts between trusses and panels are possible if the high torques associated to the original actuator have been maintained. Consequently, the solution is to apply a ‘softer’ actuation law, in the sense of preventing such contact.

The problems associated with the unfolding of an isotropic flexible model due to the actuator deployment law have been identified by Anantharaman and Hiller [1991], and the solution found was to modify that actuation in order to prevent the wrong deployment mechanism, which is in essence similar to the solution adopted here. When using composite material models, the problem of the first phase of the unfolding process increases in importance not only because the bending of the panels is significant but also because torsional modes come in play. In Figure 8 the variation of the actuator angle during the simulation period for the composite models is presented.

Figure 8 shows that the two models lead to similar simulation results. However, it is observed that after the equilibrium positions are reached for both models, in the period from 7 to 8 s, the direction of rotation of the truss members of the panels made with the lay-up 1 is opposite to that of the same truss members of the model made with lay-up 2. This discrepancy can result from the difference between the vibration modes of the both models. In fact, the lay-up 1 has no layers with the 90° orientation, thus the stiffness of this model in the Y direction is smaller than that observed with lay-up 2. A similar difference in stiffness is also visible in the X direction of the lay-up 1.

When observing the fourth frame of the unfolding in Figure 9a, it can be noticed that the flexible model of the satellite antenna predicts interference between panel 2 and panel 1, which is attached to the base satellite, when bodies B_7 and B_8 get aligned. This can be perceived as a flaw in the design of the unfolding process of the satellite that requires being fixed. If not detected, the interference would cause impact between the panels eventually leading to their failure.

6.3. Optimization of the SAR antenna. In this section the multibody model of the SAR antenna is used within the framework of an optimization problem. The flexibility of the panels of the SAR antenna is fundamental for the functional requirements of the antenna. The use of stiffer panels can improve the

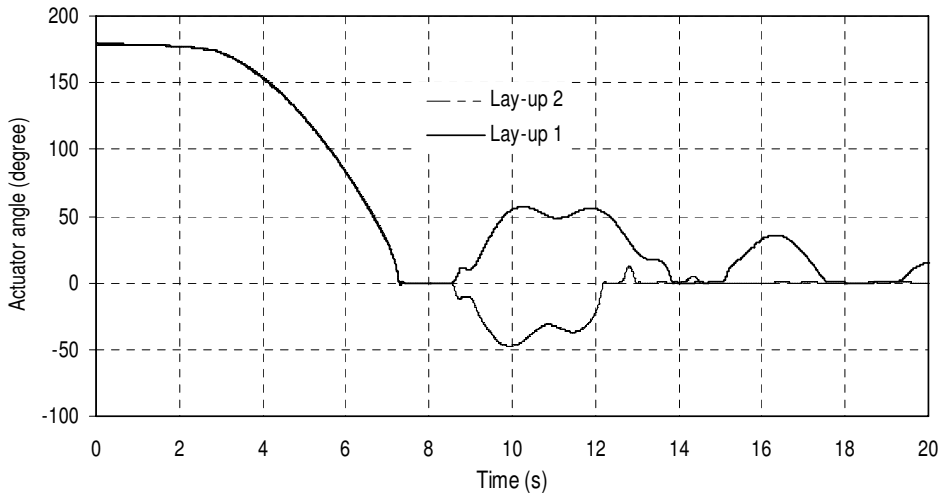


Figure 8. Actuator angle during the first phase of deployment for different composite material lay-ups.

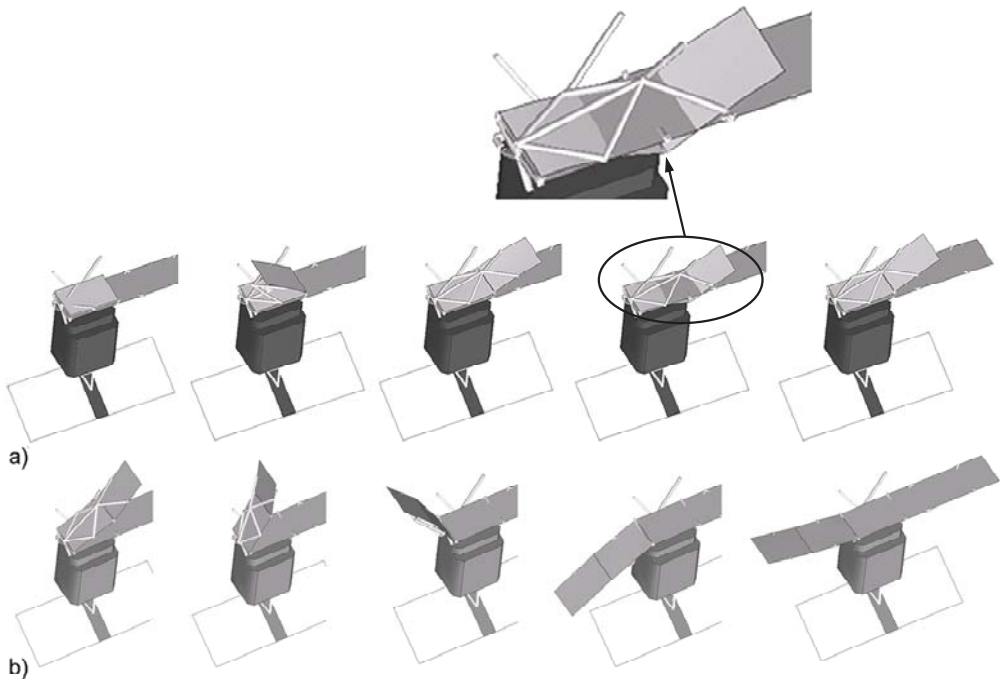


Figure 9. Configuration of the antenna unfolded process: a) first phase b) second phase.

Panels	Design Variable	Lower Bound	Initial Value	Upper Bound
2 = 3	$\theta_1/\theta_2/\theta_2/\theta_1$	$-90^\circ/-90^\circ/-90^\circ/-90^\circ$	$55^\circ/-55^\circ/-55^\circ/55^\circ$	$+90^\circ/+90^\circ/+90^\circ/+90^\circ$

Table 4. Design variables for panels' layers' orientations in the satellite optimization.

time needed to unfold the antenna, during the first phase of the unfolding process, allowing for the use of a stiffer actuator on revolute joint R_3 . Furthermore, the stiffness increase of the panels, in particular of panel 2, prevents the interference detected between panels in the first part of the unfolding process.

The multibody model of the flexible antenna for the first part of the unfolding process is composed of two flexible panels. Therefore, the antenna deformation energy of the panels for instant t_n is defined as

$$\begin{aligned}
 2U_m(\mathbf{w}_i, t_n) &= \sum_{i=2}^3 \mathbf{w}_i^T \mathbf{X}_i^T \mathbf{K}_{ff}^i \mathbf{X}_i \mathbf{w}_i \\
 &= \sum_{i=2}^3 \mathbf{w}_i^T \boldsymbol{\Lambda} \mathbf{w}_i = 2(U_2(\mathbf{w}_2, t_n) + U_3(\mathbf{w}_2, t_n)),
 \end{aligned} \tag{33}$$

where the index m refers to the model used and index i refers to the body number of panels of the multibody model SAR antenna. Equation (33) indicates that the deformation energy of the multibody model of the SAR antenna is obtained as a summation of the deformation energy of the two panels of the model. Then the function $f_0 = 2U_m$ is used to optimize the SAR antenna.

The goal defined by Equation (29) represents an area defined by the curve of function $f_0 = 2U_m$ during the simulation period $t_i = 0 \text{ s} \leq t \leq t_e = 3 \text{ s}$. The minimum value of the area may be achieved with a peak value of the maximum deformation energy of each panel that exceeds acceptable limits. In order to avoid this situation, the maximum value of the deformation energy, in each panel, is constrained to be

$$\Psi_i(\boldsymbol{\theta}) \leq c_i; \quad i = 2, 3. \tag{34}$$

The values c_i are defined as being the maximum values of deformation energy, in each panel, observed in the initial design. Therefore, in the initial design the optimization algorithm has two active constraints.

All material models considered herein are symmetric laminates with the number of layers being fixed. The simulation scenario considered is restricted to the first three seconds of the unfolding process, identified as the critical period. Two design variables are used in the optimization process, corresponding to the orientation of the layers that make up the laminate used to model panels 2 and 3. The initial design of laminate used in the panels is defined in Table 4. The optimization method used is the Modified Method of Feasible Directions (MMFD), as available in DOT [Vanderplaats 1992]. The analytic sensitivities computed by the direct differentiation method are used to compute the gradients required by the optimizer.

In Table 5 the optimization results are presented for the flexible multibody of the antenna. In Figure 10 the evolution of the objective function for the antenna flexible multibody model is showed, the progress of the design variables being shown in Figure 11. Figure 12 shows the actuator angle history during the first phase of the unfolding antenna for the original and optimum designs.

	Panel 2 (MFD)	Panel 3 (MFD)
Optimum <i>Layer orientations</i>	1.06°/−47°/−47°/1.06°	
Initial <i>objective function</i>	0.0219814	
Optimum <i>objective function</i>	0.00097180	
Reduction of <i>objective function</i>	95.6%	
Number of Constraints	2	
Number of Design Variables	2	
Active Constraints	0	
Active Side Constraints	0	
Function Calls	14	
Gradient Calls	4	
Number of Iterations	4	

Table 5. Summary of the optimization results of the satellite on the second optimization scenario.

In Figure 10 it is possible to verify that the optimization procedure converges very fast to the optimum solution, reducing the deformation energy on the order of 95%. The largest variation in the design variables observed is associated with the outside layers of the laminate, as depicted in Figure 11. The deformation energies of panels 2 and 3 are compared for the initial and the optimized models of the panels 2 and 3 in Figures 13 and 14, respectively. By observing the initial and optimized deformation energy of panels 2 and 3 it is possible to conclude that the major contribution to the reduction of the deformation energy is verified in panel 2.

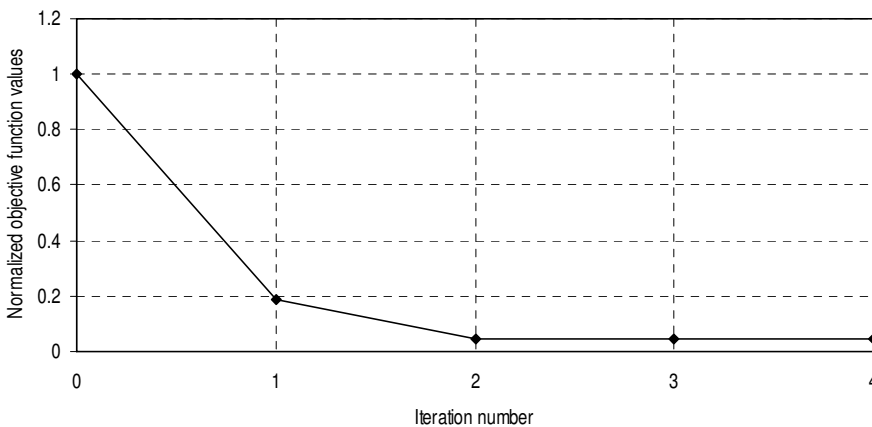


Figure 10. Evolution of the objective function during the optimization process.

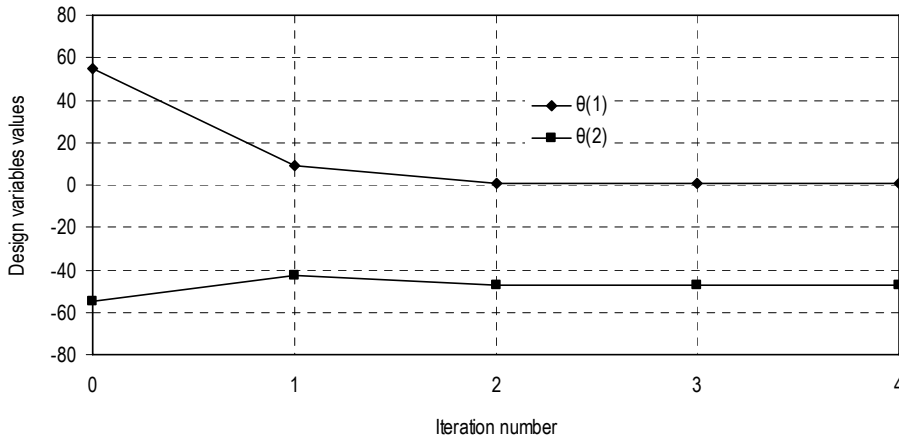


Figure 11. Evolution of the design variables during the optimization process.

7. Conclusions

A general method for the design optimization of flexible multibody systems made of composite materials has been presented in this work and demonstrated by an application to the design of the unfolding process of a satellite antenna. First, the correct choice of the optimization methods and the optimal problem definition is more complex when the nonlinear dynamic response of the systems is involved. Furthermore, the need to use analytic sensitivities instead of numerical sensitivities requires that expeditious methods of obtaining these are implemented in order to allow for the definition of more general objective functions, constraints and design variables. This has been achieved in this work by using an automatic differentiation tool to obtain the gradients required by the optimizer. Finally, the optimization of the nonlinear dynamic systems in general, and of the flexible multibody systems in particular, often present time-dependent

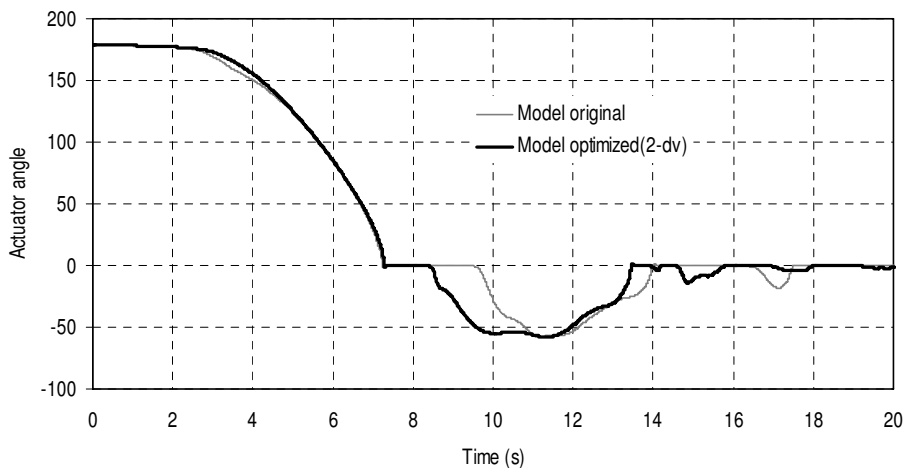


Figure 12. Actuator angle for the initial and optimum laminate of the antenna panels.

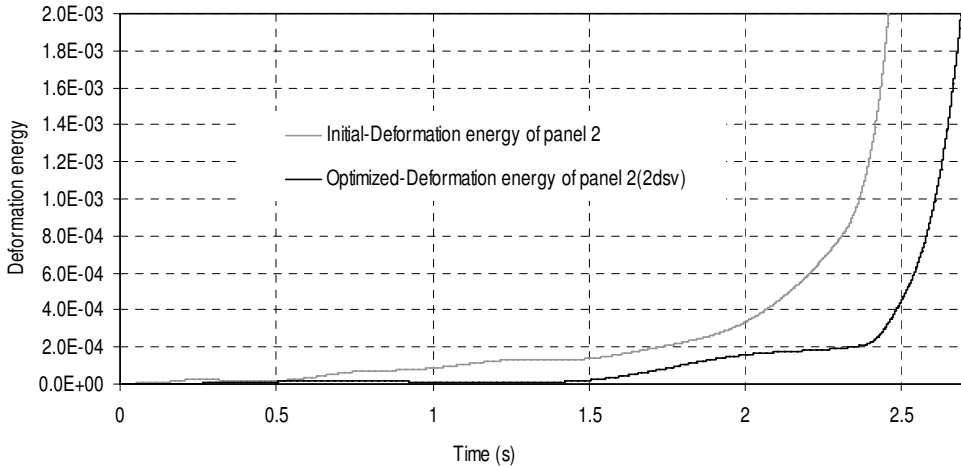


Figure 13. Deformation energy for the initial and optimum model of panel 2.

constraints that are difficult to tackle with common procedures. The use of min-max optimization is a form of handling most optimization problems of this type.

The application of the methodology developed for a complex system was demonstrated by considering the multibody model of the SAR antenna. The optimization method was applied to minimize the deformation energy of the SAR antenna panels. To get a stiffer antenna, the optimization problem was formulated as minimization problems of the deformation energy of each panel. The design variables of the optimization problem were the fiber orientations of the layers that form the lamination used to model the material properties of the panels. The design problem considers the case of finding optimum symmetric lamination with four layers only. In the optimization scenario two design variables were used to define the optimum lamination on both panels. The results of this application demonstrate that not

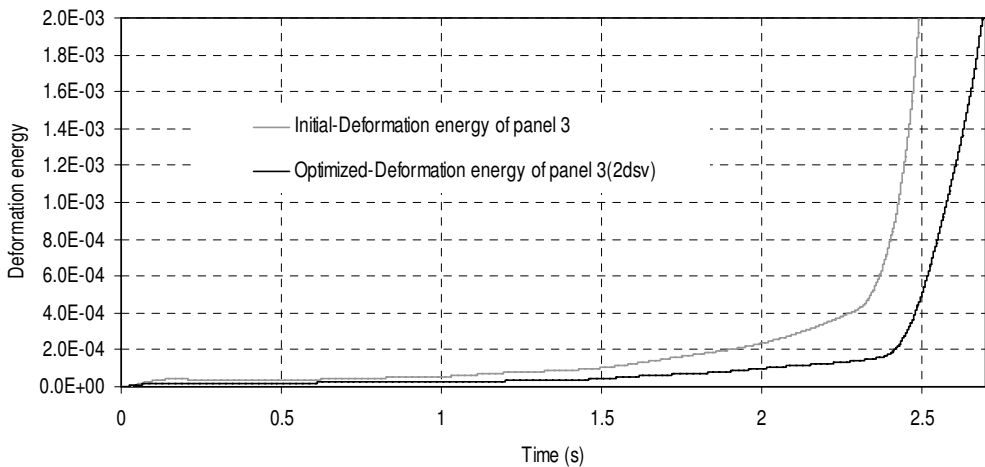


Figure 14. Deformation energy for the initial and optimum model of panel 3.

only are there feasible designs for the antenna in which interference between panels is avoided but also that the control over of the deformation energy of the antenna was possible. In the process it was shown that feasible designs for the actuation law during the deployment are obtained.

Acknowledgements

We would like to thank Professors Manfred Hiller and Andrés Kecskeméthy, of the University of Duisburg, Germany, for providing the necessary data to model the SAR antenna and for useful discussions.

References

- [Ambrósio 1996] J. Ambrósio, “Dynamics of structures undergoing gross motion and nonlinear deformations: a multibody approach”, *Comput. Struct.* **59**:6 (1996), 1001–1012.
- [Ambrósio 2003] J. Ambrósio, “Efficient kinematic joint descriptions for flexible multibody systems experiencing linear and non-linear deformations”, *Int. J. Numer. Methods Eng.* **56**:12 (2003), 1771–1793.
- [Ambrósio and Gonçalves 2001] J. Ambrósio and J. Gonçalves, “Complex flexible multibody systems with application to vehicle dynamics”, *Multibody Syst. Dyn.* **6**:2 (2001), 163–182.
- [Anantharaman and Hiller 1991] M. Anantharaman and M. Hiller, “Numerical simulation of mechanical systems using methods for differential-algebraic equations”, *Int. J. Numer. Methods Eng.* **32**:8 (1991), 1531–1542.
- [Bischof et al. 1992] C. Bischof, A. Carle, G. Corliss, A. Griewank, and P. Hovland, “ADIFOR: generating derivative codes from fortran programs”, *Sci. Program.* **1**:1 (1992), 11–29.
- [Bischof et al. 1996] C. Bischof, P. Khademi, A. Mauer, and A. Carle, “ADIFOR 2.0: automatic differentiation of Fortran 77 programs”, *IEEE Comput. Sci. Eng.* **3**:3 (1996), 18–32.
- [Bottasso et al. 2006] C. Bottasso, A. Croce, B. Savini, W. Sirchi, and L. Trainelli, “Aero-servo-elastic modeling and control of wind turbines using finite-element multibody procedures”, *Multibody Syst. Dyn.* **16**:3 (2006), 291–308.
- [Cavin and Dusto 1977] R. Cavin and A. Dusto, “Hamilton’s principle: finite-element methods and flexible body dynamics”, *AIAA J.* **15**:12 (1977), 1684–1690.
- [Chang and Nikravesh 1985] C. Chang and P. Nikravesh, “Optimal design of mechanical systems with constraint violation stabilization method”, *J. Mech. Transm. (Trans. ASME)* **107** (1985), 493–498.
- [Cook 1987] R. Cook, *Concepts and applications of finite element analysis*, 2nd ed., Wiley, New York, 1987.
- [Dailey 1989] R. L. Dailey, “Eigenvector derivatives with repeated eigenvalues”, *AIAA J.* **27**:4 (1989), 486–491.
- [Dmitrochenko et al. 2006] O. Dmitrochenko, W.-S. Yoo, and D. Pogorelov, “Helicoseir as shape of a rotating string I): 2D theory and simulation using ANCF”, *Multibody Syst. Dyn.* **15**:2 (2006), 135–158.
- [Duff et al. 1986] I. Duff, A. Erisman, and J. Reid, *Direct methods for sparse matrices*, Clarendon Press, Oxford [Oxfordshire], 1986.
- [Eberhard et al. 1999] P. Eberhard, W. Schiehlen, and D. Bestle, “Some advantages of stochastic methods in multicriteria optimization of multibody systems”, *Arch. Appl. Mech.* **69**:8 (1999), 543–554.
- [Eberhard et al. 2003] P. Eberhard, F. Dignath, and L. Kübler, “Parallel evolutionary optimization of multibody systems with application to railway dynamics”, *Multibody Syst. Dyn.* **9**:2 (2003), 143–164.
- [Gerstmayr and Schöberl 2006] J. Gerstmayr and J. Schöberl, “A 3D finite element method for flexible multibody systems”, *Multibody Syst. Dyn.* **15**:4 (2006), 305–320.
- [Gonçalves and Ambrósio 2005] J. Gonçalves and J. Ambrósio, “Road vehicle modeling requirements for optimization of ride and handling”, *Multibody Syst. Dyn.* **13**:1 (2005), 3–23.
- [Grandhi et al. 1986] R. Grandhi, R. Haftka, and L. Watson, “Design-oriented identification of critical times in transient response”, *AIAA J.* **24**:4 (1986), 649–656.

- [Haftka and Gürdal 1992] R. Haftka and Z. Gürdal, *Elements of structural optimization*, 3rd rev. exp. ed., Kluwer Academic Publishers, Dordrecht, 1992.
- [Hardeman et al. 2006] T. Hardeman, R. G. K. M. Aarts, and J. B. Jonker, “A finite element formulation for dynamic parameter identification of robot manipulators”, *Multibody Syst. Dyn.* **16**:1 (2006), 21–35.
- [Haug and Arora 1979] E. Haug and J. Arora, *Applied optimal design: mechanical and structural systems*, Wiley, New York, 1979.
- [He and Mcphee 2005] Y. He and J. Mcphee, “Multidisciplinary optimization of multibody systems with application to the design of rail vehicles”, *Multibody Syst. Dyn.* **14**:2 (2005), 111–135.
- [Heckmann et al. 2005] A. Heckmann, M. Arnold, and O. Vaculík, “A modal multifield approach for an extended flexible body description in multibody dynamics”, *Multibody Syst. Dyn.* **13**:3 (2005), 299–322.
- [Hiller 1983] M. Hiller, *Mechanische systeme*, Springer-Verlag, Berlin, Germany, 1983.
- [Hsieh and Arora 1984] C. Hsieh and J. Arora, “Design sensitivity analysis and optimization of dynamic response”, *Comput. Methods Appl. Mech. Eng.* **43**:2 (1984), 195–219.
- [Kim and Choi 1996] M. Kim and D. Choi, “A new approach to the min-max dynamic response optimization”, pp. 65–72 in *IUTAM-symposium on optimization of mechanical systems* (Stuttgart, 1996), edited by D. Bestle and W. Schiehlen, Kluwer, Dordrecht, 1996.
- [Kübler et al. 2005] L. Kübler, C. Henninger, and P. Eberhard, “Multi-criteria optimization of a hexapod machine”, *Multibody Syst. Dyn.* **14**:3–4 (2005), 225–250.
- [Lehner and Eberhard 2006] M. Lehner and P. Eberhard, “On the use of moment-matching to build reduced order models in flexible multibody dynamics”, *Multibody Syst. Dyn.* **16**:2 (2006), 191–211.
- [Liu et al. 2007] J.-F. Liu, J. Yang, and K. Abdel-Malek, “Dynamics analysis of linear elastic planar mechanisms”, *Multibody Syst. Dyn.* **17**:1 (2007), 1–25.
- [Møller et al. 2005] H. Møller, E. Lund, J. Ambrósio, and J. Gonçalves, “Simulation of fluid loaded flexible multibody systems”, *Multibody Syst. Dyn.* **13**:1 (2005), 113–128.
- [Neto 2005] M. Neto, *Optimization of flexible multibody systems with composite materials*, Ph. D. Thesis, Mechanical Engineering Department of Coimbra University, Coimbra, Portugal, 2005.
- [Neto et al. 2004] M. Neto, J. Ambrósio, and R. Leal, “Flexible multibody systems models using composite materials components”, *Multibody Syst. Dyn.* **12**:4 (2004), 385–405.
- [Nikravesh and Lin 2005] P. Nikravesh and Y.-S. Lin, “Use of principal axes as the floating reference frame for a moving deformable body”, *Multibody Syst. Dyn.* **13**:2 (2005), 211–231.
- [Pereira and Proença 1991] M. Pereira and P. Proença, “Dynamic analysis of spatial flexible multibody systems using joint co-ordinates”, *Int. J. Numer. Methods Eng.* **32**:8 (1991), 1799–1812.
- [Vanderplaats 1992] G. Vanderplaats, “DOT-Design Optimization Tools, Version 3.0”, VMA Engineering, Colorado Springs, CO, 1992.
- [Venkataraman and Haftka 1999] S. Venkataraman and R. Haftka, “Optimization of composite panels: a review”, in *Proc. of the 14th annual technical conference of the american society of composites*, Technomic Publishing, Dayton, OH, Sep. 27–29 1999.
- [Venkataraman and Haftka 2002] S. Venkataraman and R. Haftka, “Structural optimization: what has Moore’s law done for us?”, in *43rd AIAA/ASME/ASCE/AHS/ASC structures structural dynamics and materials conference*, Denver, CO, 22–25 April 2002.
- [Vetyukov et al. 2006] Y. Vetyukov, J. Gerstmayr, and H. Irschik, “Modeling spatial motion of 3D deformable multibody systems with nonlinearities”, *Multibody Syst. Dyn.* **15**:1 (2006), 67–84.
- [Yoo and Haug 1986] W. Yoo and E. Haug, “Dynamics of flexible mechanical systems using vibration and static correction modes”, *J. Mech. Transm. (Trans. ASME)* **108** (1986), 315–322.

JORGE A. C. AMBRÓSIO: jorge@dem.ist.utl.pt

Instituto de Engenharia Mecânica — Instituto Superior Técnico, Technical University of Lisbon, Av. Rovisco Pais, 1041-001, Lisbon, Portugal

MARIA AUGUSTA NETO: augusta.neto@dem.uc.pt

Departamento de Engenharia Mecânica, Faculdade de Ciência e Tecnologia da Universidade de Coimbra (Polo II), 3020 Coimbra, Portugal

ROGÉRIO PEREIRA LEAL: rogerio.leal@dem.uc.pt

Departamento de Engenharia Mecânica, Faculdade de Ciência e Tecnologia da Universidade de Coimbra (Polo II), 3020 Coimbra, Portugal

